Effective Internal Impedance Method for Series Impedance Calculations of Lossy Transmission Lines: Comparison to Standard Impedance Boundary Condition

Sangwoo Kim, Beom-Taek Lee[#], Emre Tuncer[*], and Dean P. Neikirk

Electrical Engineering Research Laboratory

Department of Electrical and Computer Engineering

The University of Texas at Austin

Austin, TX 78712

Abstract

A new impedance boundary condition method for calculating the series impedance of lossy quasi-TEM transmission lines is presented. Previous techniques using a more standard impedance boundary condition are typically limited to high frequency where the impedance boundary conditions can be easily approximated due to its localized characteristics in that limit. The new impedance boundary condition, referred to as the effective internal impedance (EII) produces values that are relatively localized (independent of the presence of other conductors) from low to high frequency, allowing the relatively simpler surface impedance of an isolated conductor to be used as an approximation of the EII.

#: current address: Intel Corporation, 2111 NE 25th Ave, M/S: JF1-207, Hillsboro, OR 97124

*: current address: Monterey Design Systems, 894 Ross Drive, Suite 200 Sunnyvale, CA 94089-1443

corresponding author:

Dean P. Neikirk, FAX: (512) 47104669, e-mail: neikirk@mail.utexas.edu

I. Introduction

For efficient modeling of wide bandwidth, high speed lossy transmission lines frequency dependent characteristics induced by finite metal conductivity must be accurately approximated. One of the more popular approaches is the "volume filament technique" [1, 2], where the conductor volume is divided into several filaments each assumed to carry uniform currents; under this assumption it is straightforward to calculate the mutual inductances between these filaments (Fig. 2a). The inverse of impedance matrix can then be obtained. However, due to highly non-uniform current distributions at high frequency, a large number of filaments must be used to accurately predict series impedance when skin and proximity effects are strong. A generally more attractive approach is a "surface integral equation method" [3, 4] where only surface currents are modeled, requiring much less memory usage and CPU time for simulation. This approach, however, requires calculation of surface current distributions using the method of moments that can be numerically expensive, especially when there are sharp corners. This technique may also have numerical problems at low frequency when current distribution is almost uniform across the cross-section of the conductors, as opposed to the high frequency limit when the current density is well approximated as a surface current.

An impedance boundary condition (IBC) is usually adopted to simplify the problem by eliminating the regions with finite conductivity from the domain to be solved, for example, the lossy conductors in eddy current and transmission line problems [5]. Solutions can then be obtained by applying the finite element method (FEM) [6, 7], the boundary element method (BEM) [8, 9], the electric/magnetic field integral method (MFIE/EFIE) [10, 11], the finite difference time domain method (FDTD) [12, 13], etc.

Schelkunoff [14] first introduced the concept of surface impedance for the analysis of coaxial cables. A simple and widely used boundary condition, the Leontovich boundary condition [15] (referred to here as the standard impedance boundary condition (SIBC)),

was originally developed for use when the skin depth is small relative to other dimensions of the problem, or the layer is thin and highly lossy. At low and mid frequency where the skin depth is comparable to or larger than the dimensions of the structures, the surface impedance is strictly no longer a local property and depends on the global geometry of the conductors. Consequently it is much harder to approximate surface impedance at low frequencies. The new technique presented in this paper shows a new boundary condition whose properties are much easier to predict over a broad bandwidth from low to high frequency.

II. Motivation and Formulation

The volume filament technique has been widely used in high performance package modeling since an external Green's function can be used to calculate mutual inductances between conductors regardless of their different conductivities, avoiding solving complicated boundary condition problems that are often encountered in surface equivalent problems. Also, this technique directly calculates resistances and inductances (rather than field quantities) that are frequently required for circuit simulation. According to the equivalence theorem, the original problem can be replaced with equivalent surface currents as long as this current generates the correct fields outside of the conductors, while the fields inside of the conductor can be assumed to be arbitrary. This allows one to replace the medium inside the conductor boundaries with the same medium as the external region. Consequently, an external Green's function can be used everywhere in the integral equations.

In formulating a surface boundary condition the fields inside of the conductor are usually assumed to be zero [16], but here we assume the vector magnetic potential is continuous across conductor surfaces, and the equivalent surface current is defined as the difference between original tangential magnetic field and internal tangential magnetic field generated in this new equivalent problem. Figure 1 shows the original problem and the

equivalent problem explained here. Of course, it might seem that this new approach would make problem much more complicated, but as will be demonstrated in this paper, the surface impedance boundary condition satisfying this new problem, the effective internal impedance (EII), is much more localized than the SIBC from low to high frequencies. The surface integral equation before applying the equivalence theorem for the exterior region can be obtained from [3]

$$\oint dr' G_{ext}^1(r,r')\,\mu H_t(r') + \oint dr' \left[G_{ext}^2(r,r') - p(r')\delta(r-r')\right] A_z(r') = 0 \quad , \tag{1}$$

where H_t and A_z are the tangential magnetic field and longitudinal magnetic vector potential respectively, $p(r')$ is the position dependent coefficient describing source strength distribution (often assumed without justification to be 0.5), and G_{ext}^1 and G_{ext}^2 are the free space external Green's function and its derivative with respect to the surface normal, respectively, and the integral is carried out along the perimeter of all conductors. For the interior region,

$$\oint_{\Gamma_q} dr' G_q^1(r,r')\, j\omega\mu H_t(r') - \oint_{\Gamma_q} dr' \left[G_q^2(r,r') + \left[1 - p(r')\right]\delta(r-r')\right] E_z(r') = 0 \quad , \tag{2}$$

where G_q^1 and G_q^2 are the Green's function and its normal derivative for conductor q, respectively, and the integral is carried out along the each individual conductor perimeter Γ_q. Equation (1) and (2) have to be solved together with the requirement that

$$\oint_{\Gamma_q} dr' H_t = I_q \quad , \tag{3}$$

where I_q is the total current carried by conductor q.

After applying the equivalence theorem, the Green's function that appears in equation (2) can be replaced by the free space Green's function used in (1). In this paper we use continuity of the vector magnetic potential across conductor surfaces to complete the definition of the EII. Equation (1) for the exterior region becomes

$$\oint dr' G^1_{ext}(r,r')\,\mu H^{ext}_t(r') + \oint dr' \left[G^2_{ext}(r,r') - p(r')\delta(r-r')\right] A_z(r') = 0 \quad , \tag{4}$$

where H_t^{ext} is the external tangential magnetic field. For the interior region equation (2) becomes

$$\oint dr' G^1_{ext}(r,r')\,\mu H^{in}_t(r') + \oint dr' \left[G^2_{ext}(r,r') + [1-p(r')]\delta(r-r')\right] A_z(r') = 0 \quad , \tag{5}$$

where H_t^{in} is the internal tangential magnetic field and the integral is now carried out along the entire surface of inside of the conductor.

If the values of external tangential magnetic field and magnetic vector potential are exactly known in equation (4) (here, magnetic vector potential is related to magnetic field by $\vec{A} = \nabla \times \mu \vec{H}$), the position dependent coefficient $p(r')$ can be determined, and then H_t^{in} can be found from equation (5).

For this new equivalent problem, the relationship between the longitudinal electric field and the difference of the tangential magnetic fields across the equivalent surface impedance sheet is called the effective internal impedance (the EII, to distinguish it from the SIBC), and is then

$$Z_{eii}(\omega, r') = \frac{E_z(r')}{H^{ext}_t(r') - H^{in}_t(r')} = \frac{E_z(r')}{J_s(r')} \quad , \tag{6}$$

where Z_{eii} is the EII and J_s is the equivalent surface current density.

To compute the integrated quantities of series impedance using the EII approach, power applied, power dissipated, and magnetic energy stored in the equivalent problem are found using

$$-\int_S ds \nabla \Phi^q \cdot \vec{J}^*_s = \int_S ds Z_{eii} |J_s|^2 + j\omega \int_S ds \vec{A} \cdot \vec{J}^*_s \quad , \tag{7}$$

where S is the conductor surface and Φ is the electric potential. The left-hand side of the equation (7) is the power applied, the first term of right-hand side is the power dissipated,

and the second term corresponds to the magnetic energy stored. From the power dissipation term in (7), resistance can be calculated using

$$R_q^{srm}(\omega) = \frac{\oint_{\Gamma_q} dr' \,\mathrm{Re}\left\{ Z_{eii} |J_s|^2 \right\}}{\left| \oint_{\Gamma_q} dr' J_s \right|^2} \cdot l_q \quad , \tag{8}$$

where l_q is the length of the line q. Internal inductance of conductor q and total external inductance are calculated from the stored magnetic energy term,

$$\begin{aligned} L_{in,q}^{srm}(\omega) &= \frac{\mu \int_{V_q} dv \, \vec{H}^{in} \cdot \vec{H}^{in\,*}}{|I_q|^2} = -\frac{\int_{S_q} ds \, \hat{n} \cdot \left(\vec{A} \times \vec{H}^{in\,*} \right)}{\left| \oint_{\Gamma_q} dr' J_s \right|^2} \\ &= -\frac{\oint_{\Gamma_q} dr' \,\mathrm{Im}\left\{ E_z H_t^{in*} \right\}}{\omega \left| \oint_{\Gamma_q} dr' J_s \right|^2} \cdot l_q \end{aligned} \tag{9}$$

and

$$\begin{aligned} L_{ext}^{srm}(\omega) &= \frac{\mu \int_{V_{ext}} dv \, \vec{H}^{ext} \cdot \vec{H}^{ext\,*}}{\sum_{q=1}^{m} |I_q|^2} = \frac{\int_{S} ds \, \hat{n} \cdot \left(\vec{A} \times \vec{H}^{ext\,*} \right)}{\sum_{q=1}^{m} \left| \oint_{\Gamma_q} dr' J_s \right|^2} \\ &= \sum_{q=1}^{m} \left(\frac{\oint_{\Gamma_q} dr' \,\mathrm{Im}\left\{ \left(E_z + \nabla \Phi^q \right) H_t^{ext*} \right\}}{\omega \left| \oint_{\Gamma_q} dr' J_s \right|^2} \right) \cdot l_q \quad , \end{aligned} \tag{10}$$

where V_{ext} is the volume exterior to the conductors. The surface inductance due to the magnetic energy stored by the impedance sheet is given by

$$L_{sur,q}^{srm}(\omega) = \frac{\int_S ds \,\mathrm{Im}\left\{ Z_{eii}^q |J_s|^2 \right\}}{\omega \left| I_q \right|^2} = \frac{\oint_{\Gamma_q} dr' \,\mathrm{Im}\left\{ Z_{eii}^q |J_s|^2 \right\}}{\omega \left| \oint_{\Gamma_q} dr' J_s \right|^2} \cdot I_q \quad . \tag{11}$$

Finally, the sum of internal, external, and surface inductances from (9), (10), and (11) gives the total series inductance for the transmission line in the EII formulation.

To validate equations (8) to (11), a similar procedure can be used to derive the equations for series impedance using the boundary element method [3, 17]. Using the exact exterior magnetic and electric fields from the original problem, it can be shown that the resistances given by (8) are identical to the original problem, that the external inductance given by (10) is identical to the original problem, and the sum of (9) and (11) is identical to the internal inductances in the original problem.

III. Surface Ribbon Method

For series impedance calculation, even though (8) to (11) are useful to validate the new approach, it is a time-consuming task to solve the coupled integral equations. A much simplified formulation can be derived directly from (4), (5), and (6). By subtracting (5) from (4) and applying (6) the following integral equation results for m conductor system.

$$\sum_{q=1}^{m} \oint_{\Gamma_q} dr' \left\{ j\omega\mu G_{ext}^1 + \delta(r-r') Z_{eii}(r') \right\} J_s(r') + \sum_{q=1}^{m} \oint_{\Gamma_q} dr' \delta(r-r') \nabla_z \Phi^q = 0 \quad . \tag{12}$$

Each conductor perimeter Γ_q can be further divided into N_q segments, each with sub section $C_{q,k}$, where these pieces represent current-carrying "ribbons" of width $w_{q,k} = \int_{C_{q,k}} dr$. Equation (12) then becomes

$$Z_{eii}^{q,k}(r) J_s^{q,k}(r) + j\omega\mu \sum_{i=1}^{m} \sum_{j=1}^{N_i} \int_{C_{i,j}} dr' \, J_s^{i,j}(r') \, G_{ext}^1(r,r') = -\nabla_z \Phi^{q,k}, \tag{13}$$

where $Z_{eii}^{q,k}$ and $J_s^{q,k}$ are respectively, the effective internal impedance and sheet current density on the k[th] ribbon ($k = 1,2,\cdots,N_q$) of the q[th] conductor ($q = 1,2,\ldots,m$) at a given frequency, and the second term on the left hand side represents contributions from self and mutual inductances. For a two dimensional case $G_{ext}^1(r,r') = -\frac{1}{2\pi}\ln|r-r'|$. If the ribbons are narrow enough that the sheet current density is constant across each ribbon, integrating over the k[th] ribbon yields

$$\frac{I_s^k}{w_k}\int_{C_k} dr Z_{eii}^k(r) + j\omega\mu\sum_{i=1}^{N}\frac{I_s^i}{w_i}\int_{C_k}\int_{C_i} dr'\,dr G_{ext}^1(r,r') = -\int_{C_k} dr\nabla_z\Phi^k \quad , \tag{14}$$

where I_s^k is the total sheet current carried by the k[th] ribbon, and for simplicity the double superscript (q,k) has been replaced with the single superscript k ($k = 1,2,\ldots,N$, $N = N_q \times m$). Finally,

$$\overline{Z_{eii}^k}\, I_s{}^k\,\frac{l_k}{w_k} + j\omega\mu\sum_{i=1}^{N}\frac{I_s^i\, l_k}{w_k\, w_i}\int_{C_k}\int_{C_i} dr'dr G_{ext}^1(r,r') = \Phi_1^k - \Phi_2^k \quad , \tag{15}$$

where Φ_1^k - Φ_2^k is voltage drop along the ribbon k, $\overline{Z_{eii}^k}$ is the EII averaged over the width of ribbon k, and l_k is the length of ribbon k, which is assumed to be 1 in a two dimensional problem. Equation (15) can be expressed as an N x N matrix equation

$$\left[\left(\left[Z_{eii}\right] + j\omega[L]\right)\right]\cdot[I] = [V] \tag{16}$$

where $\left[Z_{eii}\right]$ is an N x N diagonal matrix made up of the $\overline{Z_{eii}^k}/w_k$ and $[L]$ is a matrix consisting of self and mutual inductances between surface ribbons. This approach is called the surface ribbon method (SRM); Fig. 2b illustrates the technique for rectangular conductor. Now rather than calculating resistance and inductance from equation (8) to (11), if $\left[Z_{eii}\right]$ is known (16) can be used to calculate resistance and inductance directly, as is done in the volume filament method [1, 2]. As shown in the following section, the EII has relatively localized characteristics, allowing $\left[Z_{eii}\right]$ to be easily approximated.

IV. Sample Results

To calculate the exact EII, the volume filament technique can be used to find the external magnetic and electric fields and the vector magnetic potential, then these values can be used in (4) and (5) to calculate the internal magnetic field, and finally the EII is found using (6). Fig. 3 shows a comparison between the EII values for two circular conductors with radii 1 mm separated by 0.2 mm, 20 mm, and 200 mm, and the surface impedance of an isolated circular conductor given by [18],

$$Z_{cir} = \frac{j\sqrt{j\omega\mu\sigma}}{\sigma}\frac{J_0\left(ja\sqrt{j\omega\mu\sigma}\right)}{J_1\left(ja\sqrt{j\omega\mu\sigma}\right)}\ , \tag{17}$$

where a is the radius of the conductor. The most interesting characteristics of the EII is the position independence of the real part at low frequency, as shown in Fig. 3a. All real parts of the EII are almost constant and are quite close to the surface impedance of the isolated conductor calculated from (17). The imaginary parts do have a position dependence, especially when two conductors are very close to each other. However, this dependence diminishes quickly as the two conductors are separated, with values of Im(EII) being approximately the average of that obtained from (17). At high frequency, the internal fields of the conductors approach zero, and the EII calculated from (6) is expected to approach to the SIBC which is accurately approximated by (17) in the high frequency limit. Fig. 3b shows that this does indeed occur. In other words, (17) can be used as an approximation of the EII to calculate series impedance of circular conductors regardless of the frequency or proximity of other conductors (i.e., $\overline{Z_{eii}^{k}} \approx Z_{cir}$ in (15) and (16)). To support this point, the series impedance of two circular conductors separated by 0.2 mm is calculated and compared with the volume filament method as shown in Fig. 4. Here, a polygon with degree 24 shown in Fig. 4a is used instead of a circular conductor to simplify the calculation of the mutual inductance between ribbons. Figure 4b indicates (17) is indeed a

good approximation of the EII for series impedance calculation even when conductors are very close to each other.

The EII values for square conductors with width 25 μm and separated by 5 μm and 50 μm have also been calculated. It is impossible to calculate exactly the SIBC of isolated square or rectangular conductors due to the singularity at the corner, however, it can be approximated [19-21]. Fig. 5 shows the low frequency characteristics of the EII. Both real and imaginary parts of the EII show similar characteristics as the circular case except near the corner. At high frequency, the surface impedance of an infinitely wide and thick conductor given by

$$Z_s = \sqrt{\frac{\pi f \mu}{\sigma}}(1+j) \tag{18}$$

is a reasonable approximation for the SIBC far from corners; Fig. 6 shows that the EII also approaches (18) except near the corner. Examination of other geometrical cases has confirmed that the EII is well approximated by the surface impedance of an isolated conductor, regardless of the presence of other conductors. Various studies [17, 22] have shown that an approximated EII can be directly applied to (16) to accurately estimate the series impedance of various cross-sectional conductors. The series impedance calculations for multi-conductor transmission lines using the SRM are detailed in [17, 22].

V. Conclusions

The precise definition of an alternative surface impedance boundary condition has been formulated for use in lossy transmission line analysis. For this boundary condition, the conductor is modeled as an impedance sheet on the conductor perimeter, the conductor interior is replaced by a (non-conducting) exterior material, and the effective internal impedance (EII) is defined on the impedance sheet. At low frequency, the real part of the EII is almost constant along the perimeter of a conductor, and at high frequency the EII approaches the SIBC; hence, the EII is approximately a local quantity from low to high

frequency. Approximations to the EII can be used in the surface ribbon method, producing numerically efficient and accurate calculation of the series impedance of lossy multi-conductor lines. Here, the SRM was applied to two dimensional problems, but can be extended to three dimensional problems [17]. Since this method requires substantially less memory than the VFM, the SRM can be used effectively for ground plane modeling including current crowding effects.

Acknowledgements: This work was sponsored by the Defense Advanced Projects Agency (DARPA) under grant number AFOSR F49620-96-1-0032.

References

[1] A.E. Ruehli, "*Inductance Calculations in a Complex Integrated Circuit Environment,*" IBM Journal of Research and Development, vol. Sept.,1972, pp.470-481.

[2] W.T. Weeks, *et al.*, "*Resistive and inductive skin effect in rectangular conductors,*" IBM J. Res. and development, vol. 23 ,1979, pp.652-660.

[3] M.J. Tsuk and J.A. Kong, "*A Hybrid Method for the Calculation of the Resistance and Inductance of transmission Lines with Arbitrary Cross Sections,*" IEEE Transactions on Microwave Theory and Techniques, vol. 39 August,1991, pp.1338-1347.

[4] R.-B. Wu and J.-C. Yang, "*Boundary Integral Equation Formulation of Skin Effect Problems In Multiconductor Transmission Lines,*" IEEE Transactions on Magnetics, vol. 25 July,1989, pp.3013-3015.

[5] D.J. Hoppe and Y. Rahmat-Samii, *Impedance Boundary Conditions in Electromagnetics*. A SUMMA Book. 1995: Taylor & Francis.

[6] A. Darcherif, *et al.*, "*On the use of the surface impedance boundary concept in shielded and multiconductor cable characterization by the finite element method,*" IEEE Transactions on Magnetics, vol. 28 March,1992, pp.1446-1449.

[7] J. Jin, *The Finite Element Method in Electromagnetics*. 1993: John Wiley & Sons, Inc.

[8] E.M. Deely, "*Avoiding surface impedance modification in BE methods by singularity-free representations,"* IEEE Transactions on Magnetics, vol. 28 September,1992, pp.2814-2816.

[9] T.H. Fawzi, M.T. Ahmed, and P.E. Burke, "*On the use of impedance boundary conditions in eddy current problems,"* IEEE Transactions on Magnetics, vol. 21 September,1985, pp.1835-1840.

[10] J.R. Mosig, "*Arbitrary shaped microstrip structures and their analysis with a mixed potential integral equation,"* IEEE Transactions on Microwave Theory and Techniques, vol. 36 February,1988, pp.314-323.

[11] B.J. Rubin, "*An electromagnetic approach for modeling high-performance computer packages,"* IBM Journal of Research and Development, vol. 34 July,1990, pp.585-600.

[12] J.H. Beggs, *et al.*, "*Finite-difference time-domain implementation of surface boundary conditions,"* IEEE Transactions on Antennas and Propagation, vol. 40 January,1992, pp.49-56.

[13] J.G. Maloney and G.S. Smith, "*The use of surface impedance concepts in the finite-difference time-domain method,"* IEEE Transactions on Antennas and Propagation, vol. 40 January,1992, pp.39-48.

[14] S.A. Schelkunoff, "*The electromagnetic theory of coaxial transmission lines and cylindrical shields,"* Bell System technical Journal, vol. 13 ,1934, pp.532-579.

[15] M.A. Leontovich, *On the approximate boundary conditions for electromagnetic fields on the surface of well conducting bodies*. Investigations of Propagation of Radio Waves. 1948, Moscow, USSR: Printing house of the Academy of Sciences. 5-20.

[16] A.R. Djordjevic, T.K. Sarkar, and S.M. Rao, "*Analysis of finite conductivity cylindrical conductors excited by axially-independent TM electromagnetic field,"* IEEE Transactions on Microwave Theory and Techniques, vol. 33 October,1985, pp.960-966.

[17] B.-T. Lee, "*Efficient Series Impedance Extraction Using Effective Internal Impedance,"*, in *Electrical and Computer Engineering*. 1996, The University of Texas at Austin: Austin.

[18] S. Ramo, J.R. Whinnery, and T.V. Duzer, *Fields and Waves in Communication Electronics*. 2nd ed. 1984, New York: Wiley.

[19] E.M. Deely, "*Surface Impedance Near Edges and Corners in Three-dimensional media,"* IEEE Transactions on Magnetics, vol. 26 March,1990, pp.712-714.

[20] E.M. Deely, "*Improved impedance boundary condition for finite elements by cross-coupling at corners,"* IEEE Transactions on Magnetics, vol. 30 ,1994, pp.2881-2884.

[21] W. Jingguo, J.D. Lavers, and Z. Peibai, "*Modified Surface Impedance Boundary Condition Applied to Eddy Current Problems,"* IEEE Transactions on Magnetics, vol. 28 March,1992, pp.1197-1200.

[22] E. Tuncer, B.-T. Lee, and D.P. Neikirk. *Interconnect Series Impedance Determination Using a Surface Ribbon Method*. in *IEEE 3rd Topical Meeting on EPEP*. 1994. Monterey, CA.

Figure Captions

Figure 1: (a) Original problem where conductors with finite conductivity carry volume currents. (b) equivalent problem where conductor interior is replaced with non-conducting exterior medium and equivalent surface current satisfying the boundary condition is used.

Figure 2: (a) Illustration of the volume filament technique where L_{ij} represents the self ($i = j$) and mutual ($i \neq j$) inductances between filaments; R is filament resistance given by $1/\sigma A$ where A is the cross-sectional area of the filament. (b) Surface ribbon method where L_{ij} represents the self and mutual inductance between surface ribbons and Z_{eii} is the diagonal elements of $[Z_{eii}]$ given in (16).

Figure 3: Position dependency of EII for circular conductor with a = 1mm, d = 0.2, 20, and 200 mm. solid line: d = 0.2 mm, dotted line: d = 2 mm, dashed line: d = 200 mm, dot-dash line: equation (17). (a): low frequency limit (1 kHz); (b): high frequency limit (1 MHz).

Figure 4: (a) Segmentation scheme for circular conductor using polygon of degree 24 in the SRM. (b) Series impedance calculation of two closely spaced circular conductors with a = 1 mm, d = 0.2 mm, N = 48. Solid line: SRM; dashed line: VFM

Figure 5: Position dependency of EII for square conductor with 25 μm width and d = 5 μm and 50 μm at f = 1kHz. solid line: d = 5 μm, dashed line: d = 50 μm. (a) real part (b) imaginary part.

Figure 6: Position dependency of EII for square conductor with 25 μm width and d = 5 μm and 50 μm at f = 1 GHz. solid line: d = 5 μm, dotted line: d = 50 μm, dashed line: equation (18). (a) real part (b) imaginary part.

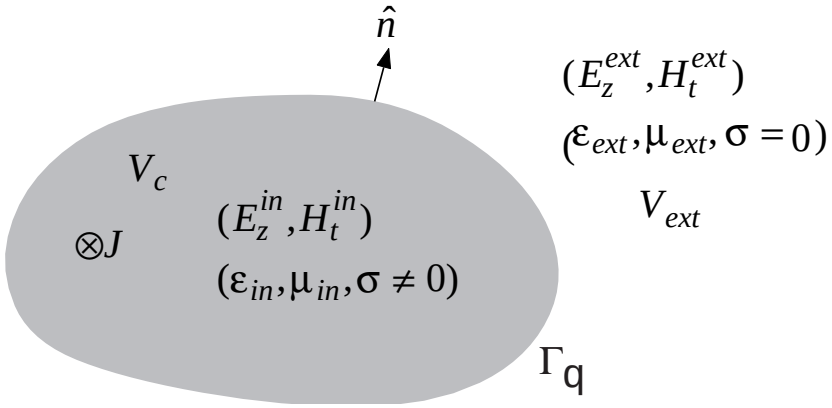
$\hat{n}$
(E_z^{ext}, H_t^{ext})
$(\varepsilon_{ext}, \mu_{ext}, \sigma = 0)$
V_{ext}
V_c
$\otimes J$
(E_z^{in}, H_t^{in})
$(\varepsilon_{in}, \mu_{in}, \sigma \neq 0)$
Γ_q

Figure 1(a)

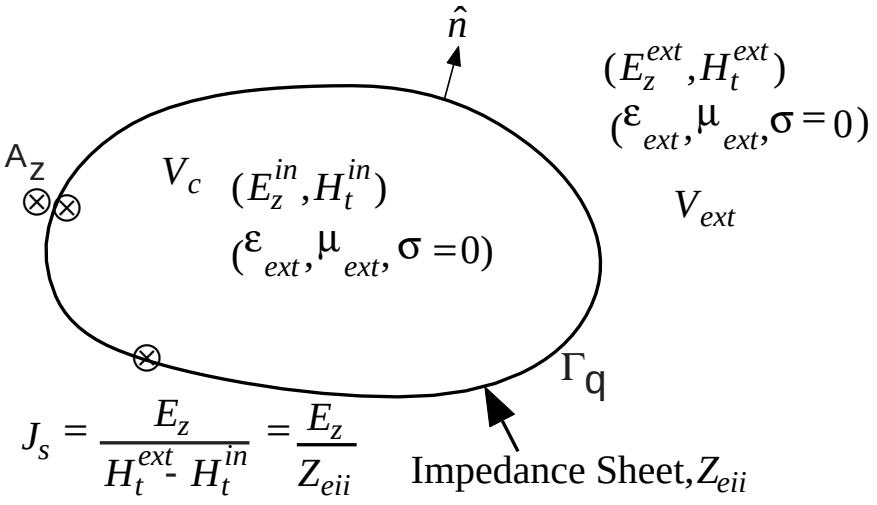
$\hat{n}$
(E_z^{ext}, H_t^{ext})
$(\varepsilon_{ext}, \mu_{ext}, \sigma = 0)$
V_{ext}
A_z
V_c
(E_z^{in}, H_t^{in})
$(\varepsilon_{ext}, \mu_{ext}, \sigma = 0)$
Γ_q
$J_s = \frac{E_z}{H_t^{ext} - H_t^{in}} = \frac{E_z}{Z_{eii}}$
Impedance Sheet, Z_{eii}

Figure 1(b)

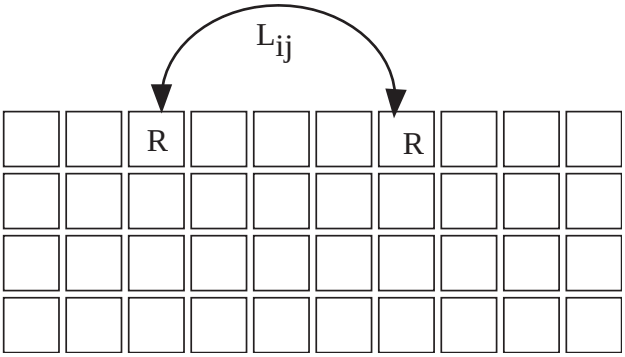

Figure 2(a)

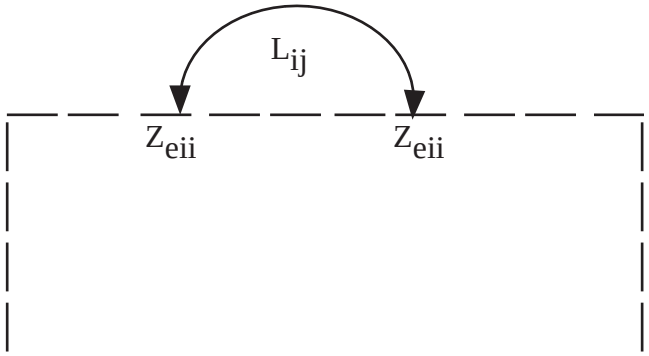

Figure 2(b)

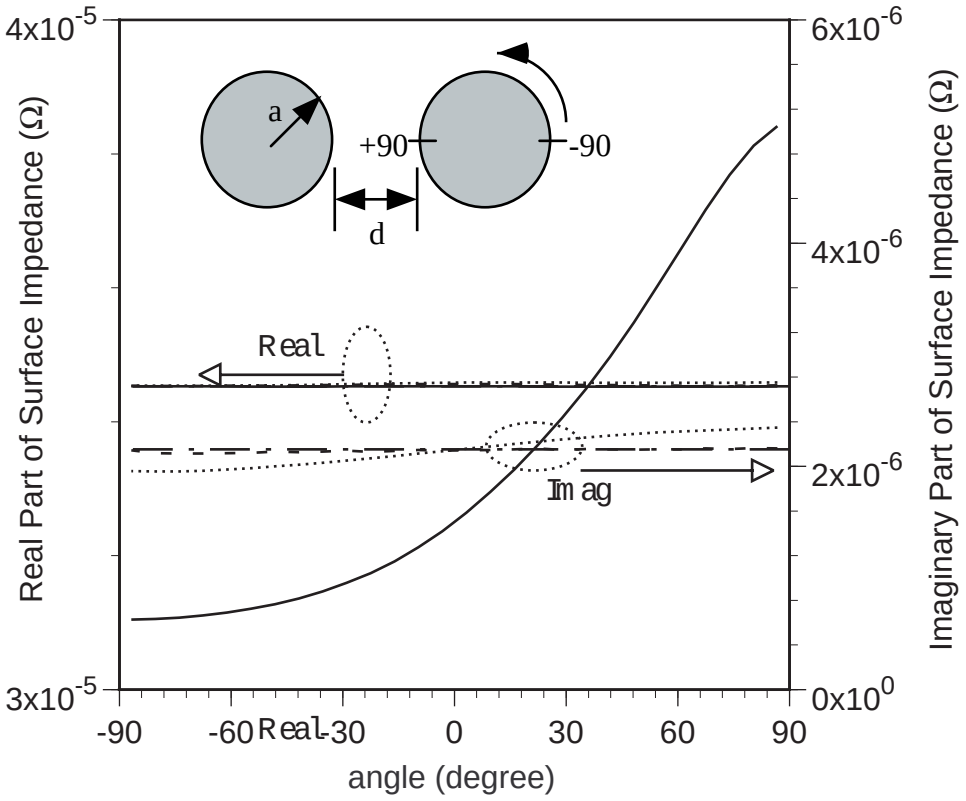
4x10-5
3x10-5
6x10-6
4x10-6
2x10-6
0x10 0
Real Part of Surface Impedance (Ω)
Imaginary Part of Surface Impedance (Ω)
a
+90
-90
d
Real
Imag
-90
-60
-30
0
30
60
90
angle (degree)

Figure 3(a)

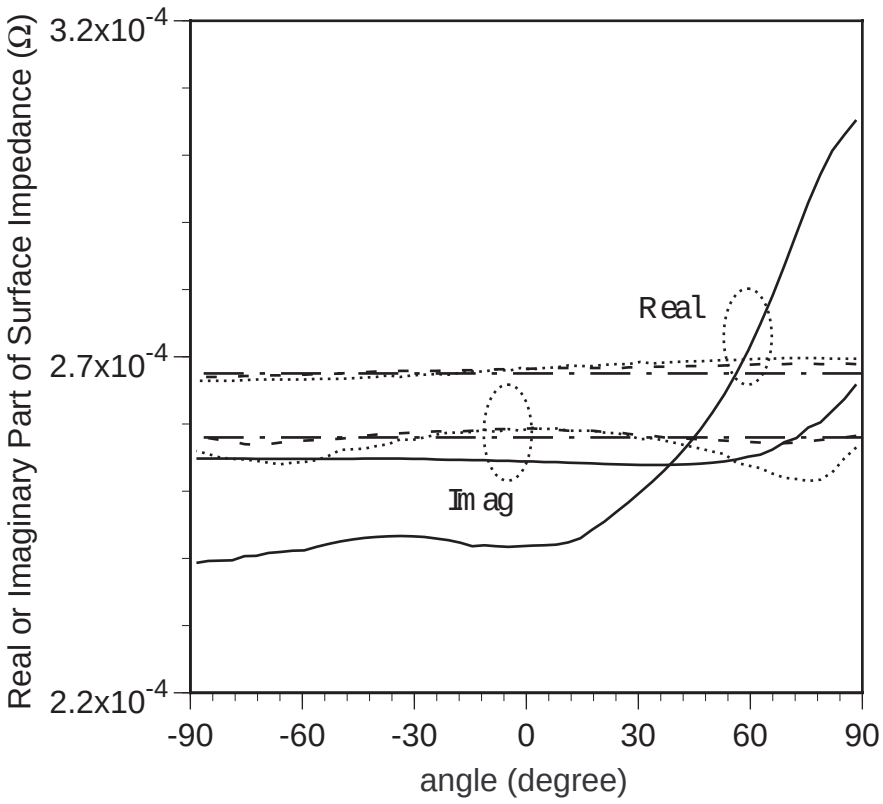
Real or Imaginary Part of Surface Impedance (Ω)
3.2x10-4
2.7x10-4
2.2x10-4
Real
Imag
-90
-60
-30
0
30
60
90
angle (degree)

Figure 3(b)

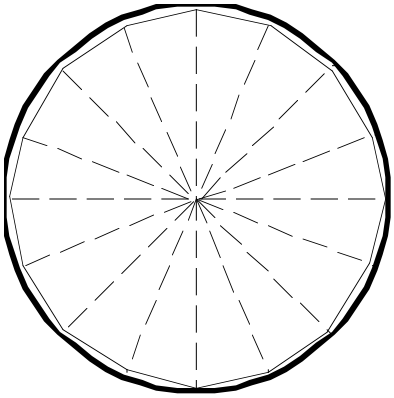

Figure 4(a)

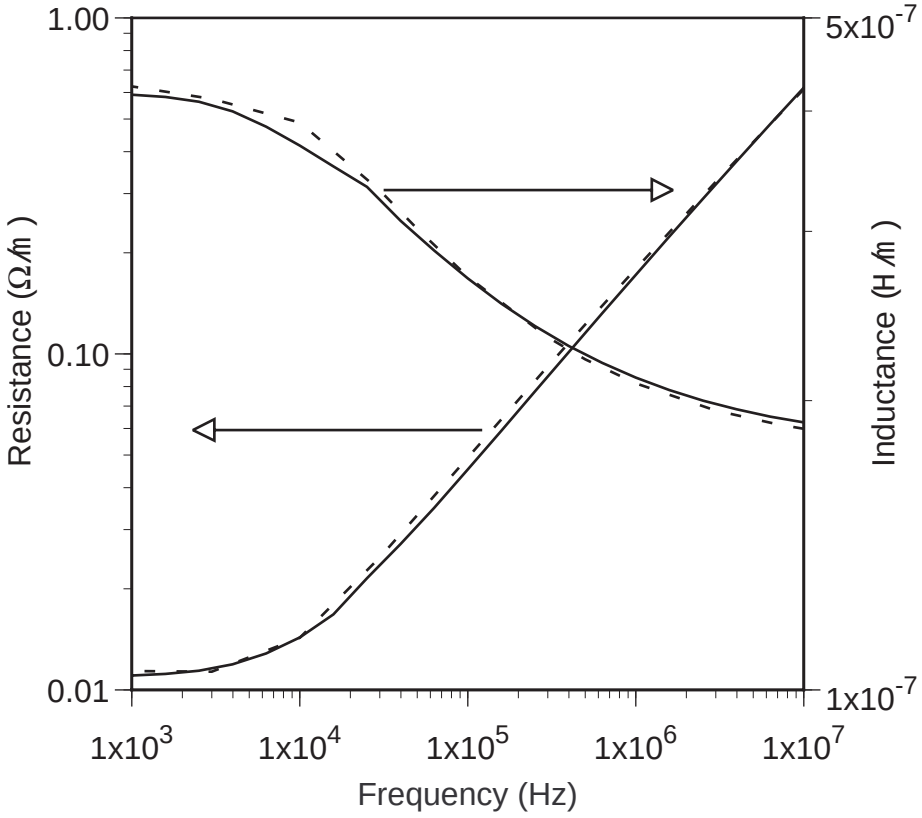
1.00
0.10
0.01
5x10-7
1x10-7
Resistance (Ω/m)
Inductance (H/m)
1x10^3
1x10^4
1x10^5
1x10^6
1x10^7
Frequency (Hz)

Figure 4(b)

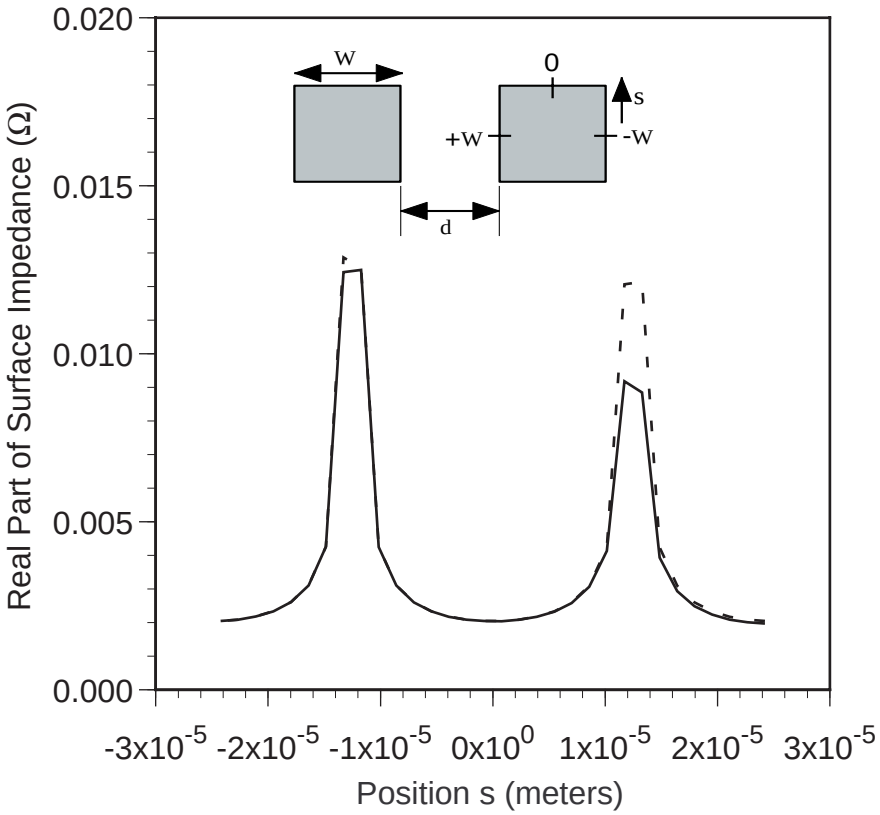
0.020
0.015
0.010
0.005
0.000
Real Part of Surface Impedance (Ω)
W
0
s
+W
-W
d
-3x10-5
-2x10-5
-1x10-5
0x100
1x10-5
2x10-5
3x10-5
Position s (meters)

Figure 5(a)

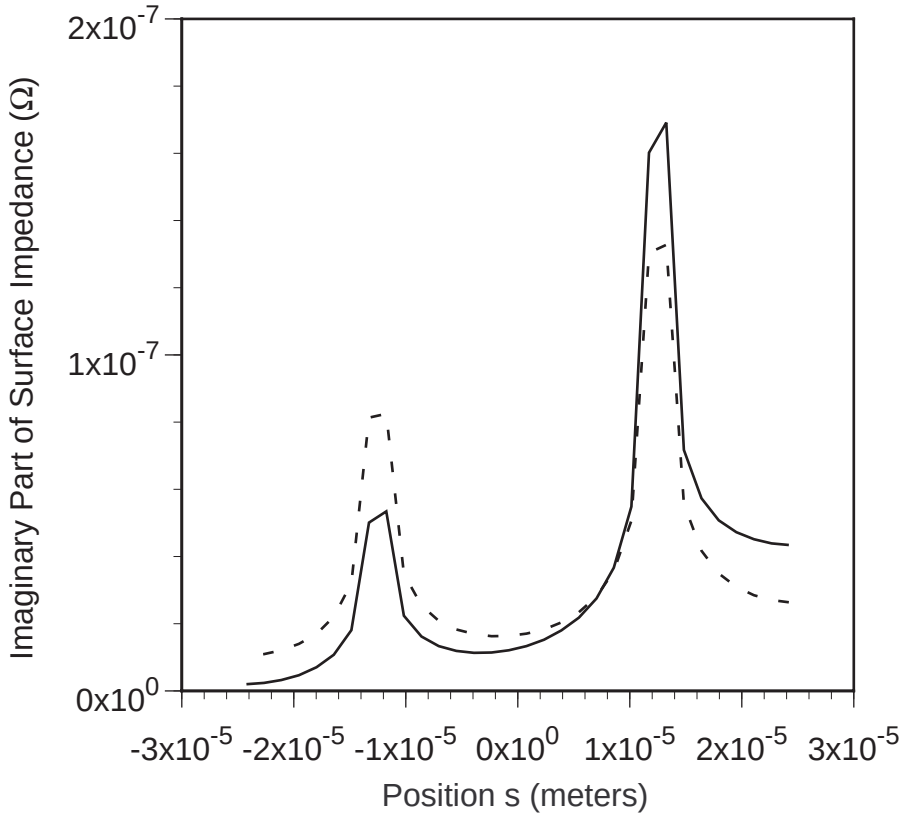
2x10-7
1x10-7
0x100
Imaginary Part of Surface Impedance (Ω)
-3x10-5
-2x10-5
-1x10-5
0x100
1x10-5
2x10-5
3x10-5
Position s (meters)

Figure 5(b)

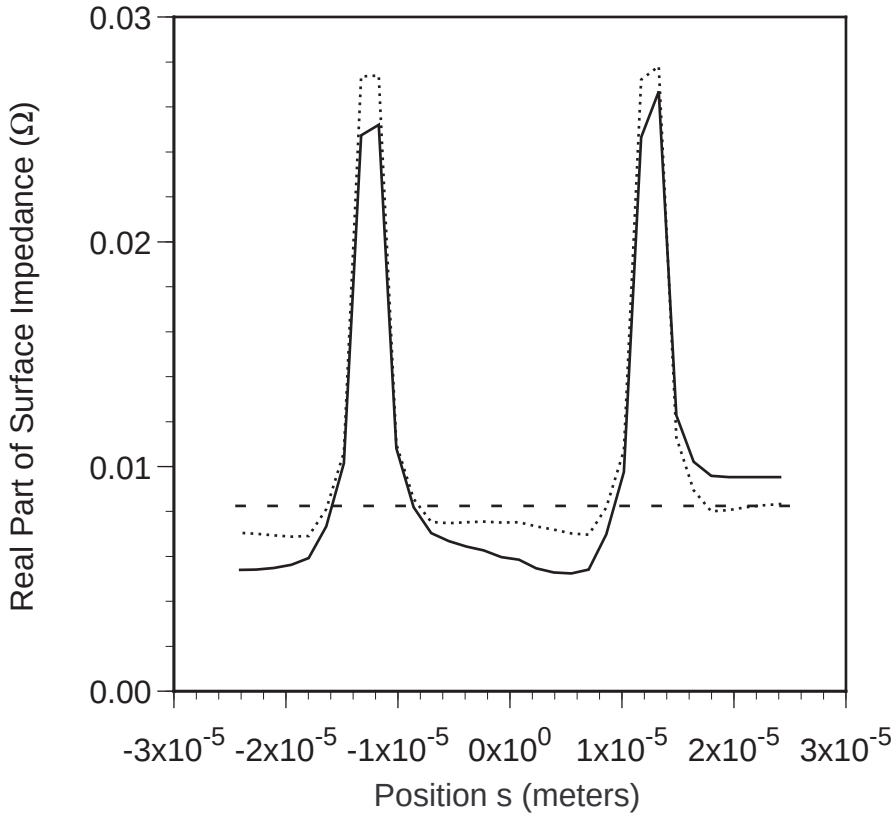
0.03
0.02
0.01
0.00
Real Part of Surface Impedance (Ω)
-3x10-5
-2x10-5
-1x10-5
0x100
1x10-5
2x10-5
3x10-5
Position s (meters)

Figure 6(a)

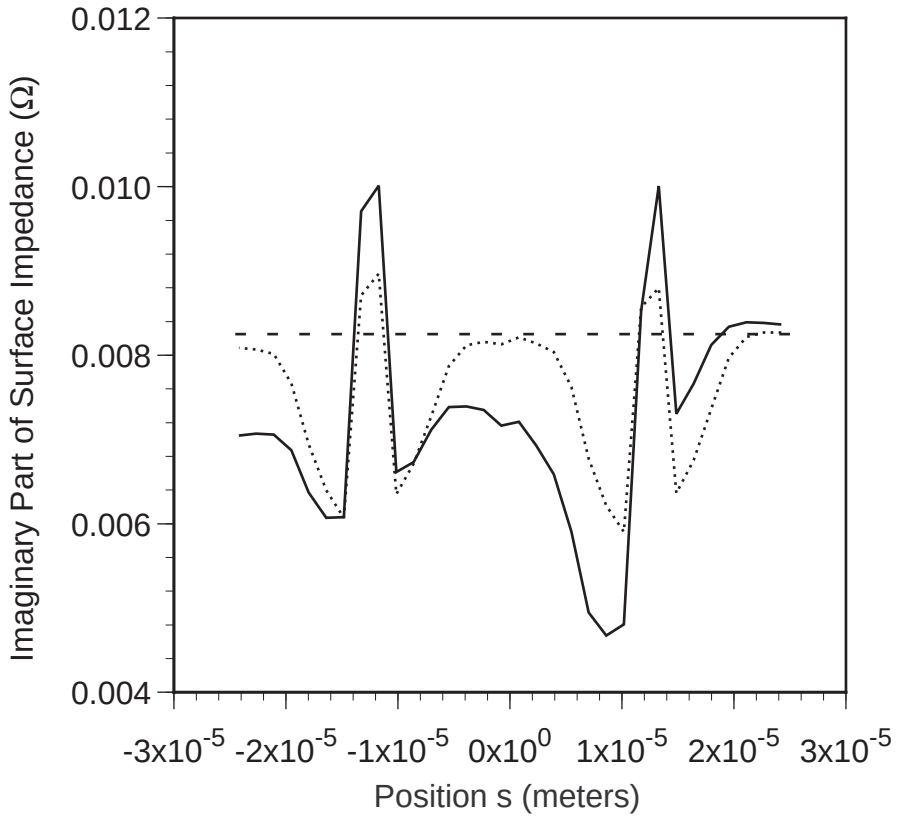
0.012
0.010
0.008
0.006
0.004
Imaginary Part of Surface Impedance (Ω)
-3x10-5
-2x10-5
-1x10-5
0x100
1x10-5
2x10-5
3x10-5
Position s (meters)

Figure 6(b)